Microfluidics on Porous Substrates Mediated by Capillarity Driven Transport

Shantimoy Kar[1#], Sankha Shuvra Das[2], Sampad Laha[2] and Suman Chakraborty[1,2]*

[1]Advanced Technology Development Centre, [2]Department of Mechanical Engineering, IIT Kharagpur, India-721302

*suman@mech.iitkgp.ernet.in

[#]Currently working as a postdoctoral research assistant in University of Glasgow, UK

Abstract: Microfluidic systems on porous substrates, including paper-based analytical platforms, have attracted significant attention in recent times, primarily attributed to their diversified applications ranging from bio-analytical devices for healthcare technologies to green energy generation and flexible electronics. In this short review, we attempt to provide a concise overview about the fundamental premises of functionalities of these devices, starting from the understanding of flow in single one-dimensional conduit. This can be extended to more complex systems, where an intrinsic capillary action offers the necessary provisions for continuous maintenance of heterogeneous flow over multiple spatio-temporal scales, which essentially facilitates the needs of specific applications. We discuss about few specific applications as demonstrative examples which are solely triggered by the intrinsic capillary action of the porous media. These specific examples delineate the fact that flexible architecture of the devices in combination with the inherent capillary driven phenomena makes it suitable to meet the desired user-specific demands at affordable costs, rendering them immensely suitable for the low resource settings environment.

Introduction

Last couple of decades have witnessed an outstanding progress in microfluidics and its technological applications in different fields of science and engineering. Microfluidics, as a subject, deals with the manipulations of fluid in microscale. Fluidic manipulations on microscale structures are controlled with the aid of different external actuations like mechanical pumps, electric field, acoustic field, magnetic valves and many others. In the context of controlled fluid manipulations over small scales, surface tension driven capillary force turns out to be an indispensable tool[1]; which may effectively be classified as 'pump-free' actuation.

Advent of microfluidics and the concept of miniaturization led to the emergence of the paradigm of 'lab-on-a-chip' with wide-spread applications in biology and chemistry. These lab-on-chip platforms are often hallmarked by an element of complexity to cater various needs like metering, valving, pumping etc. Such overwhelming complexities may be simplified to a large extent by harnessing capillarity driven manipulations[2]. Such systems can be broadly categorized into the three sections: (i) closed system, (ii) semi-open system and (iii) open system. Closed systems are those embodiments where the micro-conduits are fully enclosed. In semi-open systems, fluid inlets are usually kept open, so that fluids can be introduced through easy pipetting mechanism without necessitating conventional pumping systems. In the open microfluidic systems, fluid interacts with the ambient air during flow. The open microfluidic systems are gaining popularity for several advantages, particularly including ease of fabrication and easy handling (as the users do not need to pay attention for fluid leakage). In this short review, we aim to summarize the developments of capillarity-driven flow over microscales, from conventional capillary systems to recent advancements in porous capillary networks (e.g. paper, silk etc.). The overall discussion is structured with a specific aim of providing the detailed understanding of the underlying physical considerations and pertinent applications, with a specific focus on different analytical applications of paper-based microfluidic systems.

Although, the use of paper as a substrate for analytical testing has been in practice for centuries, its application as a microfluidic platform was first reported by Whitesides et al. in 2007[3]. Owing to different advantages like easy availability, low-cost, high effective surface area and ability to retain chemical/biological reagents, paper has been considered as an extremely suitable substrate for microfluidics-based analytical platforms. In recent times, paper-based devices have attracted significant attention in widespread applications, cutting across several specialized domains of science and technology. Till date, different analytical applications have been successfully executed using paper-based systems such as point-of-care diagnostics[4,2], water quality control (heavy metal toxicity)[5,6], food toxicity analysis[7,8], soil testing etc. From a detailed analysis, it can be realized that these analytical applications are mostly dependent on chemical/biological assays. Most often, these qualitative assays provide an optical (colorimetric, fluorescence, luminescence) signal which is further analyzed to make conclusive remarks about the assays. Further understandings of the reported literature reveal that most often these qualitative assays utilize continuous fluid transport through the matrix; while the outcome is merely affected through the microscopic heterogeneity of flow.

In the subsequent discussions, we delineate upon some of the fundamental premises of capillary driven transport in a microfluidic substrate, with paper as a specific example.

1. How Fluid Flow Occurs on Paper Matrix?

Paper is essentially composed of a random distribution of cellulose fibers. Although flow of liquid through paper is primarily guided by the inherent capillary action, the flow mechanism in such porous medium is completely different from any other capillary-based systems (e.g. glass/silicon/PDMS). Figure 1 depicts an example of a paper device where fluid flow occurs through paper pores, but not on top of the surface[9]. Microscopic view of the traversing fluid front on paper matrix illustrates that the fluid spreads randomly through the capillary network of the porous substrate. One of the most important advantages of this porous medium is its ability to wick fluid without requiring any external pumping facility. Thus, the most fundamental premises of fluid transport through paper matrix lies in capillary dynamics, which is discussed in the subsequent section.

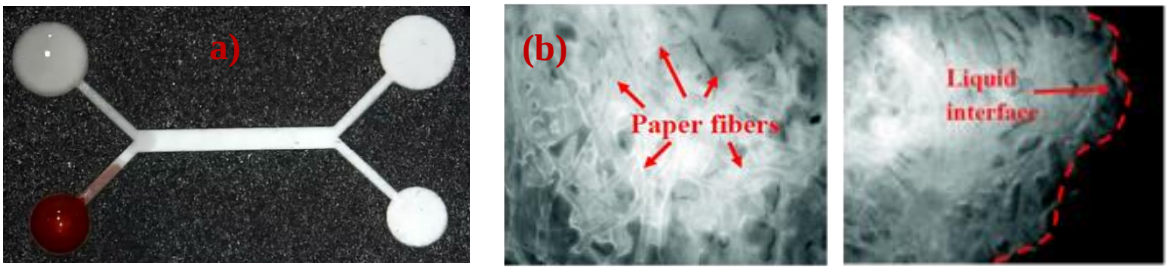

Figure 1:(a) Representative image of a paper-based device (courtesy: Microfluidics Laboratory, IIT Kharagpur, India-721302). (b) Liquid transportation through a paper matrix (captured by fluorescence microscopy; reproduced from Mandal et al.[9]).

Figure 2a shows an SEM image of Whatman filter paper, while Figure 2b represents the microstructure of a cotton cloth. From Figure 2a, it is evident that the cellulose fibers are randomly distributed on paper matrix. Though the orientations of the fibers in microscopic levels are apparently different, the fluid transport mechanisms for these systems are macroscopically similar in nature. The quality of cellulose fibers (in case of paper) and its degree of randomness is often dictated by the manufacturing process which eventually determines the porosity and thus the flow rate on the paper surface. For different grades of Whatman filter paper, the particle retention capacity varies significantly (for Grade 1: 11 μm, Grade 2: 8 μm, Grade 3: 6 μm, Grade 4: 25 μm, Grade 5: 2.5 μm, Grade 6: 3 μm, Grade 602h: < 2 μm) while the thickness of different grades remains within the range of 180-340 μm[10].

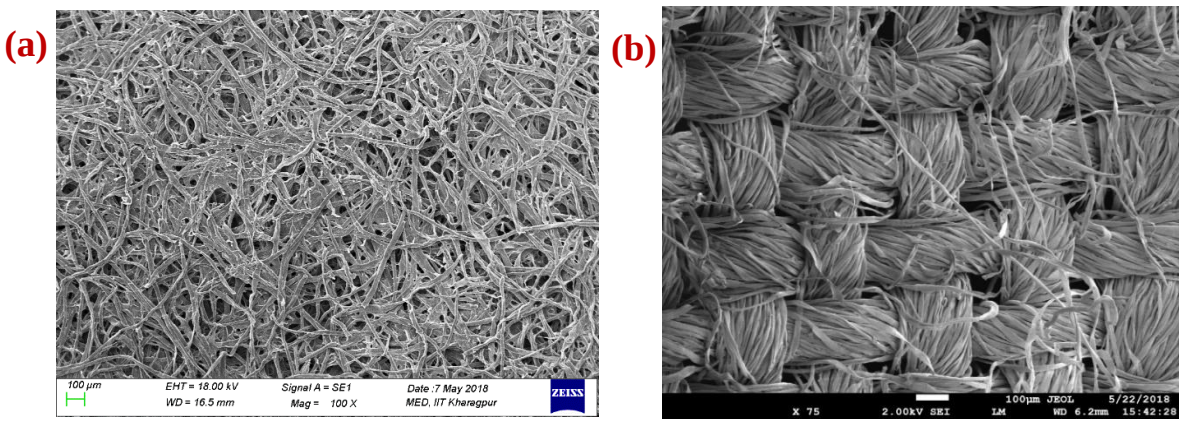

Figure 2: Scanning electron microscopic images:**(a)** Whatman grade 4 filter paper; (b) textile- (cotton) based fiber matrix (reproduced from Das et al.[55]).

2. Theoretical Perspective of Capillary Filling

2.1 Case-I: Conventional capillaries

Theoretical understanding of capillary filling mechanism has been developed long back[11,12]. In this section, we aim to discuss about the fundamental basis of capillary filling dynamics for systems ranging from a simple capillary to very complex paper-based porous networks.

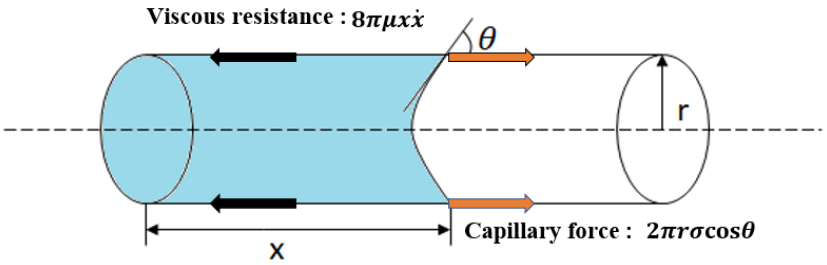

Figure 3: Schematic of capillary filling through a one-dimensional capillary

One dimensional (1D) capillary (as depicted in Figure 3) filling characteristics are well explained by the Lucas-Washburn equation[11], provided the capillary has uniform circular cross section, the reservoir volume is unlimited and gravitational as well as inertial effects are neglected. Simple force balance between the viscous and the surface tension force gives the following relation:

$$x(t) = \sqrt{\frac{r\sigma t\cos\theta}{2\mu}} \qquad (1)$$

where σ is the surface tension (liquid−vapor), μ is the dynamic viscosity of the fluid, r is capillary radius, and θ is the contact angle between the capillary wall and fluid. The above equation is valid only in the short time regime i.e. when the traversed length is smaller than the equilibrium length (H). For longer time limit i.e. when the difference between the equilibrium

length and travelled distance is tending to zero, the capillary filling dynamics follows an exponential variation:

$$x(t) = H[1 - e^{-K_2 t}] \tag{2}$$

where $K_2 = \frac{r^2 \rho g}{8\mu H}$.

Considering the contribution of inertial effects that were neglected in the previous equations, the capillary force balance equation becomes:

$$\frac{d}{dt}\left(\rho \pi r^2 x \frac{dx}{dt} + M_a\right) = 2\pi r \sigma \cos\theta - 8\pi\mu x \frac{dx}{dt} \tag{3}$$

M_a in Eq. 3 is known as the 'added mass', which is introduced to circumvent the issue of infinitely large acceleration at time, t = 0. This added mass accounts for the mass of the liquid which is just outside the inlet of the capillary and is on the verge of entering the channel[13,14]. For more in-depth analysis, consideration of dynamically evolving contact angle is preferred over the static contact angle as used in Eq. 3. From different experimental findings[15], it has been observed that, at low speeds the apparent dynamic contact angle θ_d can be described by a universal scaling relation expressed by Tanner's law[14,16]:

$$\theta_d \sim Ca^{\frac{1}{3}} \tag{4}$$

where Ca is the capillary number expressed as $Ca = \frac{\mu \ U}{\sigma}$, U denotes for the contact line velocity. As the liquid moves into the capillary, velocity decreases due to viscous effects. Accordingly, Ca also decreases, leading to the subsequent decrease in apparent contact angle according to Eq. 4. The surface tension force increases with decrease in contact angle and helps to sustain the fluid flow in the channel against the viscous force. The proportionality constant in Eq. 4 is calculated by asymptotic analysis of the thin film close to the channel wall as reported by Kalliadasis et. al[16]**.** By taking in account the effect of intermolecular forces[17] in the thin film region, Eq. 4 may be modified as[16,14]:

$$|\tan\theta_d| = 7.48\, Ca^{\frac{1}{3}} - 3.28\lambda^{0.04} Ca^{0.293} \tag{5}$$

where $\lambda = \frac{R_m}{r}$, R_m being a molecular length scale.

Dhar et. al. has reported about a universal oscillatory regime towards the end of the capillary filing process. Here, the oscillations of the liquid column about the Jurin height (i.e. the equilibrium height of liquid in a vertical capillary when the weight of liquid column is balanced by the surface tension force) have been modelled by the unique interplay between inertial and gravitational forces, in addition to the viscous and surface tension forces. The oscillations persist until the effect of inertial energy near the equilibrium height has been completely suppressed by viscous damping[18].

In diagnostic applications of microfluidic analytical devices, handling of certain physiological fluids (e.g. blood) are involved, which in general, deviate from Newtonian constitutive

behavior. The transport of blood through micro-channels has been studied by Chakraborty et al. using analytical and numerical methods, where blood has been modelled as a non-Newtonian power law fluid[14]. One interesting and non-trivial finding of that investigation is that the velocity gradient in the microchannel leads to the redistribution of the cellular components of blood and creates cell-free zone in the vicinity of the channel wall. Thus, a plasma rich layer is formed near the walls of the microchannel which causes a decrease in the apparent viscosity of whole blood, leading to greater flow rate in the channel. This effect becomes highly significant as the hydraulic radius of the channel approaches to the size of the red blood cells (RBCs) of blood, which occupies ~ 45% of total blood volume. Moreover, the velocity profile for blood seems to be blunt in comparison to the normal parabolic profile for Newtonian fluids. This observation is attributed to the phenomenon of axial accumulation of RBCs at the centerline zone leaving a plasma-rich region near the channel walls. Chakraborty and co-researchers have further described about the effect of aspect ratio of the micro channel, which plays a vital role in determining the displacement of fluid in the channel. The channel with higher aspect ratio for same height shows greater displacement of liquid into the channel at specific time instance.

2.2 Case-II: paper-based systems

We would now like to extend the basic understandings of capillary filling towards perceiving the transport characteristics on porous substrates, with a specific focus on paper-based systems. To develop a robust understanding of the flow characteristics on such porous systems, different models have been adopted and modified accordingly to explain the experimental outcomes. Lucas-Washburn (L-W) model[11] has been adopted by many research groups to describe fully saturated wet-out flow of liquid through paper-based systems. In this model, the porous system is considered as a bundle of parallel, rigid capillaries of uniform cross section. The liquid penetration length in a paper channel can be expressed as $l^2 \propto t$, where l is the traversed length at time t. The proportionality constant represents the parametric dependence of pore size and other fluidic parameters. However, the L-W model can be used only in case of one-dimensional flows in a single homogeneous porous system. Furthermore, it is also found that the L-W model is somewhat inaccurate while capturing the underlying physics at longer time scales i.e. when evaporation and swelling of cellulose fibers come into the play. Fu et al.[19] probed the flow through paper devices having non-uniform channel widths, yielding significant deviations from the LW model. To take care of these issues, many modifications have been suggested by different researchers[20,21].

Darcy's model has also been used to capture the underlying physics of capillary-driven transport through porous media, even for the case of multi-dimensional flows. Additionally, it can also be used to model flows through more than one paper like substrates connected in series[22,23]. Using this model, the volumetric flowrate (Q) through the paper substrate can be defined as

$$Q = -\frac{\kappa A}{\mu x}\Delta P \tag{6}$$

where κ is the permeability of the paper, μ is the viscosity of the fluid, A is the cross section area and ΔP is the pressure difference across the length x. In this context, it is important to

mention that alike L-W model, Darcy's model will also be valid only under the assumption of full saturation by the wetting front of liquid. However, recent studies reveal that in practical scenarios of liquid imbibition through paper, the substrate behind the wetting front remains partially saturated and this of degree of saturation varies with factors like channel geometry, properties of the membrane and that of the fluid. Walji et al.[24] experimentally demonstrated the fact that there are some pores which are not filled even in the complete wet section due to their random distribution. This phenomenon allows further absorption of liquid within the pores, thus making it an apparently filled system. Hence, Darcy's law cannot be utilized for accurate modelling in these cases.

Buser et. al[25,26] proposed a model of flow in partially saturated paper substrates by using the Richard's equation which relates the change in saturation of the porous medium with the gradient in pressure head. This can be expressed as

$$\frac{\delta\theta}{\delta t} = \frac{\delta}{\delta z}\left[K(\theta)\frac{\delta H(\theta)}{\delta z}\right] \tag{7}$$

where *K* is the hydraulic conductivity and *H* is the pressure head, both of which are functions of the volumetric water content, θ. It has been reported that the increase in saturation helps the porous medium to act as a better fluid conductor. Detailed methodologies for estimation of the hydraulic conductivity (as a function of saturation) by using the water retention curve (WRC) have been described in the doctoral dissertation of J. R. Buser[26], for different porous substrates used for paper-based microfluidic systems.

These analytical frameworks are usually applicable for straight capillaries considering negligible changes in kinetic energy and constant permeability. For analyzing fluid flow through single-layered paper-based devices with horizontal orientation, simple geometries and smaller gap heights, the above-described models are considered to be excellent approximations. These models also have one common underlying assumption that the porous media used for analysis is rigid, i.e. there is no spatio-temporal variation of the constituent material property (size of fibers, pore space between the fibers, etc.) of the medium during liquid imbibition. However, in case of paper, swelling of fibers during wicking, violates the assumption of rigid porous media and leads to dynamic alterations of the pore radius, permeability and porosity. Schuchardt et al. proposed a model of wicking in a swelled porous media by modifying the Washburn equation[27]. By incorporating the assumption of linear decrease of pore radius with time, the modified model showed better fit to the experimental findings as compared to the traditional Washburn model. Masoodi et al. have modelled the swelling phenomenon during liquid wicking by coupling Darcy's law with a modified continuity equation, characterized by source and sink terms[28]**.** Source term represents the effect of change of porosity while the sink term takes care of the liquid absorption by the fibers during swelling. Furthermore, the effect of permeability on the porosity of the medium has also been investigated to understand the corresponding effect on capillary imbibition rate.

3. **Fabrication and Flow Behaviour**

Before we discuss about important parameters which have a significant impact on flow characteristics, it is imperative to understand the intricate details of paper channels (shown in Figure 1a). It is also important to note that 'paper channels' are distinctly different than other microfluidic channels. 'Paper channels' usually mean the hydrophobic barriers created on porous paper substrates. The hydrophobic barriers guide the fluid through the hydrophilic cellulose fabrics. Table 1 gives concise overview of different fabrication protocols for realizing such hydrophobic barriers.

Table 1: Summary of the different fabrication techniques adopted for paper-based microfluidic systems

Method	**Required equipment**	**Required chemicals**	**Key shortcomings**
Photolithography[3,9,29]	Mask aligner, hot plate, mask	Photoresist	High cost, toxicity of the photoresists
Wax printer[30]	Wax printer, hot plate	Wax	Not suited for very low width (< 1 mm) structures
Plotting[31–33]	Plotter	Hydrophobic ink (PDMS, wax), marker pens, correction pens, eraser pens	Low resolution
Inkjet printing[34,35]	Inkjet printer	Hydrophobic chemicals, acrylate ink	Customize adaptation of inkjet printer
Laser printing[36,37]	Laser printer	Commercial toner	Additional heating is needed, limitations about the specified toner particles
Flexographic printing[38]	Printing instrument	Polystyrene, PDMS	High cost, cleaning step after the usage is tedious
Stamping[39]	Metallic stamp	Different types of commercial ink	Inconsistency in the results, low resolution
3D printer[40]	3D printer	3D printer resin	Resolution depends on the printer quality
Spraying[41,42]	Mask, UV light source	Commercial water repellent	Low resolution, poor uniformity
Laser cutting[43]	Laser cutter	None	Susceptible to contamination
Cutting[44,45]	Scissors, cutter	None	Dimensional accuracy is poor

Wax printing is one of the most widely used techniques for easy manufacturing of paper- based devices. The key challenge associated with this technique is that the wax diffuses in three possible directions in an equivalent manner; while vertical diffusion of molten wax is the only intended direction. To determine the dimensional accuracy of the devices, wax diffusion in the horizontal plane needs to be taken into consideration. This horizontal diffusion of wax within the paper matrix dictates the final dimensions of the device, which is relatively reduced than the actual designs. To address this issue, controlled heating for a definite time duration should be considered as one of key steps. In this regard, it is important to note that random distribution of cellulose fibers does not allow the formation of sharp hydrophobic barriers on paper unlike glass and silicon substrates. However, the flow through these non-uniform wall barriers does not affect the end applications of these devices. Most of the fabrication protocols for paper devices (as depicted in Table 1) suit well in the perspective of low-resource settings; however, all are not very well-suited for creating high-resolution microfluidic architectures.

Transport characteristics on paper-based systems are dependent on many parameters like pore radius, average porosity, evaporation rates (i.e. temperature and humidity), geometry of the channel, reservoir volume etc.[24]. Till date, Whatman chromatographic papers are the most used substrates for analytical purposes. However, it is worth mentioning that these types of papers are usually designed for the specific purpose of filtration. In their work, Walji et al.[24] have explained how fluid flow through paper depends on the machine direction along which the fibers are aligned. Flow along the direction of the machine is faster than the corresponding cross-directional flow. However, from a macroscopic view, it is extremely difficult to make distinction between these two types of fiber alignment. The experimental findings confirm that the length of the paper channel has minimal effect on the flow rate. However, the channels with thinner width show faster transport of liquid than its wider counterpart. In the following section, we elaborate our discussion with respect to three specific parameters: (i) effect of surroundings, (ii) tortuosity and (iii) substrate chemistry.

3.1: Surroundings

Both the external environment and surroundings of the channel vicinity have impact in determining the transport characteristics. To comment on the influence of surrounding environment, it can be said that experimental evidence suggests that the effect of humidity does not alter the flow characteristics significantly while the temperature affects the flow dynamics. Songok et al.[46] have delineated the fact that closed paper channels have faster flow rate than the open paper-based microfluidic systems. Flow delay is a customary requirement for the practical execution of multi-step assays. Many of the qualitative assays involve multistep processes, which could be easily achieved by incorporating necessary delay on capillarity networks[47]. In this context, Songok. et. al. introduced the concept of developing surface energy gradient on paper with a TiO_2 nanoparticle coating. Furthermore, precise time delays in flow have been achieved by introducing expansions and contractions in paper channels[48]. Younas et al.[49] explained the importance of threshold line thickness of the hydrophobic barrier for successful implementation of the device.

Hong. et al. have studied about the effect of hydrophobic boundaries on capillary imbibition through paper channels[50] They have reported that for paper channels with cut boundaries, the

flow velocity does not vary with the width of channel; however, if hydrophobic wax boundaries are present, the flow speed becomes a function of the channel width. The surface tension force acts in the reverse direction of flow at the hydrophobic boundaries, leading to flow retardation and this effect becomes more significant as the channel widths become narrower (~ 1 mm). A modified Washburn equation was also put forward by this study which models flow through narrow paper channels with wax boundaries[50]:

$$l_m(t) = k\sqrt{\left(1 + \beta \frac{d\cos\theta_b}{\phi^{1/3} w \cos\theta}\right)\frac{\sigma t}{\mu}} \tag{8}$$

where $l_m(t)$ is the imbibition length, d is the pore diameter, w is the channel width, ϕ is the porosity of paper, θ is the contact angle of the capillaries in bulk, θ_b is the contact angle on the side wax boundaries and *k* is a constant introduced to model the complexity in pore geometries.

3.2: Tortuosity

Although, in some of the simplified models, porous medium is often assumed to be comprising a bundle of parallel capillaries, the pore spaces within the substrate are never straight, i.e. perfectly inclined in the direction of the macroscopic flow. The flow passages are originally meandering in nature[51] and as a result, fluid in a porous media, often has to travel through a path which is several times longer than the shortest distance between the source and the sink in the direction of gross flow. The complexity in void space morphology is quantified by a parameter called tortuosity. In simple terms, tortuosity (τ) defined as:

$$\tau = \frac{L_e}{L}, \tag{9}$$

where L_e is the ratio of the average length of the actual flow paths and L is the straight-line length of the system in the macroscopic flux direction. Thus, with increase in tortuosity of the porous medium, the flow path becomes more complicated and naturally offers increased flow resistance. The concept of tortuosity originated with the objective of reducing the deviation between the experimental permeability data with that obtained from theoretical calculations using the capillary bundle model. Koponen et. al[52] have incorporated the effect of pore space meandering in Darcy's Law within the capillary model framework. They have introduced the tortuosity factor within the expression of permeability of the medium. Considering that axes of the capillary tubes to be inclined at an angle θ to the normal of the surface of the material, the permeability (k) have been expressed as:

$$k = \frac{\phi^3}{c\tau^2 s^2} \tag{10}$$

where ϕ is the porosity, τ is the tortuosity which can be expressed as $\frac{1}{\cos\theta}$, *s* represents the specific surface area (pore surface area per unit volume of the material) and *c* is a structural parameter which varies with the cross section of the capillaries. In a study of imbibition in mesoporous materials, Gruener et. al[53] incorporated the effects of tortuosity of the medium and reported an expression of the imbibed length as a function of time as:

$$\left(\frac{{r_o}^2}{4\tau\eta}\Delta p\right)^{\frac{1}{2}}\sqrt{t} \tag{11}$$

where r_o is the pore radius, η is the dynamic viscosity of the liquid, and Δp is the pressure difference (Laplace pressure) responsible for the liquid imbibition.

3.3: Substrate chemistry

Substrate chemistry plays a significant role in different applications due to the availability of the essential functional groups (e.g. hydroxyl, carboxylic acid) on the cellulose fabrics[54]. These functional groups offer essential characteristics to functionalize the surface for capturing different biomolecules. Furthermore, it has to be noted that the surface treatment of the paper is known to significantly alter the flow characteristics. Modification to the paper surface essentially accelerates or decelerates the fluid flow, which is evident from the water retention capacities for different paper types. Chemical modifications often lead to the redistribution of the pores rather than modifying the pore dimensions in significant extents. This redistribution of pores over the microscale structures, affects the swelling characteristics of the substrate, thereby essentially affecting the capillary transport characteristics of the substrate.

The degree of liquid absorption and wicking depends upon the wettability of the fibers. Due to the hydrophilic characteristics of pure cotton fibers, the water imbibition rate is faster than the synthetic or nylon based porous structures which are hydrophobic in nature[55]. In general, cotton-based fabric structures exhibit large density of open-ended nanopores, which assist in faster capillary action. On the other hand, synthetic or nylon based porous matrix contains dead-end nanopores, which impede the capillary movement of the liquid. The degree of wettability of different types of fibers can be determined through measuring the contact angle or by measuring the imbibition rate of liquid. According to the theory of capillarity, paper fibers with a larger pore radius should have a faster wicking rate due to low flow resistance. While for textile-based substrates, capillary rate is faster for pore radius greater than ~ 50 nm, though the presence of tortuosity in the fiber matrix tends to slow down the wicking action[56].

4. Can capillary flow be a representation of diffusive transport?

The wicking phenomenon on paper has been modelled in a diffusive dynamics study by Chaudhury et al.[57]. According to this study, the flow characteristics of liquid through the isotropically arranged random capillaries of paper is mainly dictated by diffusion. This phenomenon is analogous to the diffusion process occurring due to the random motion of molecules and can be expressed in terms of a diffusion length as $l^2 \propto t$, where l is the diffusion length and D is the proportionality constant being characterized as the diffusivity. In this study, a characteristic timescale (τ) has been derived for flow through paper matrix. It has been shown that when $t/\tau >> 1$, the flow dynamics can be approximated to follow the diffusion process. For transport of water through paper, this characteristic timescale value has been calculated as 3.65 μsec. In realistic scenario, experimental timescale varies between few seconds to minutes, rendering the validity of the diffusive transport paradigm.

5. Application of Capillarity Driven Flow on Porous Substrates

Numerous applications have been successfully attempted on paper-based devices, most of which followed standard chemical/biological assays. In this section, we specifically emphasize

upon two specific applications namely (i) blood plasma separation[58] and (ii) green energy generation[29].

Notably, on glass/poly-dimethyl siloxanes (PDMS)/silicon/polymer surfaces, fluid flow maintains uniformity in the microscale. However, on paper substrates/porous substrates, fluid flow creates an inhomogeneity within the microscopic structures of the cellulose fabrics. This inhomogeneity in fluid distribution often leads to heterogeneous distribution of ions and small molecules and serves as the underlying reason for different physical phenomena on paper substrates.

A. Blood Plasma Separation

Plasma separation from whole blood is known to be one of the key requirements for clinical laboratories for diagnostic applications. When the diagnostic assay involves a colorimetric reaction, the interference from the intense red color of the blood (mainly contributed from the red blood cells) leads to the erroneous measurements of the signals. In this context, gold standard technique involves centrifugation method; however, it is not suitable for handling very low volume (within a range of $\mu l$to nl) of samples. Furthermore, this centrifugation method demands complex instrumentation for adopting on-chip applications. There are many developments (mostly adopted in some commercial devices) involving the use of RBC specific membranes[59] which specifically filter RBCs and thus separate the plasma. Amongst other techniques, use of agglutination reagents[60], salt assisted methodology[61] and electrochemical methods[62] are popular. Kar et al., demonstrated the adoption of 'H-filter' design on paper-based systems[58] (depicted in Figure 4).

'H-filter' design was first demonstrated by Osborn et al.[63], for size-based molecular extraction from complex mixtures. In the H-filter design by Kar et al., two parallel fluid streams (namely whole blood and buffer) flow simultaneously due to capillary action. During transportation, the analytes, having lighter molecular weight, diffuse into the buffer from the blood stream. Therefore, due to diffusive transport, lighter analytes enrich the buffer stream while the cellular counterparts (particularly the red blood cells) are retained in the blood stream. The diffusion coefficient of small bio-analytes (e.g. glucose) is approximately 100 times higher than that of cells, which leads to a separation of cellular contents at the downstream part of the channels. This simple approach shows separation efficiency of ~ 75%. In summary, capillarity-driven natural imbibition on a special geometric configuration leads to efficient separation which could be integrated for the purpose of on-chip plasma separation.

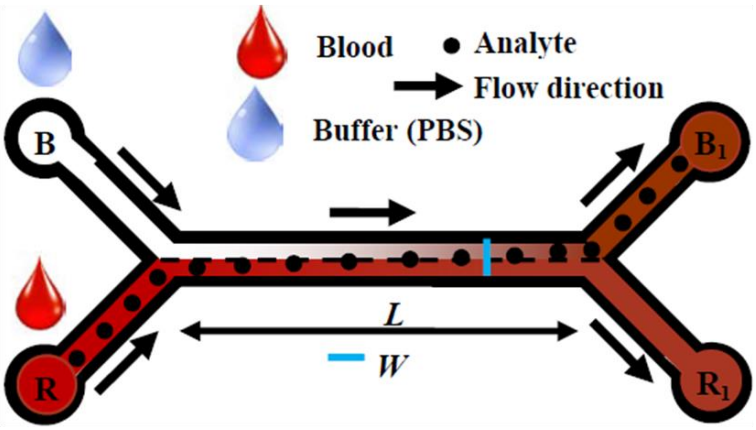

Figure 4: H-filter device, on which dilution buffer and whole blood are dispensed in reservoirs B and R, respectively. Due to diffusive transport of the low molecular weight biomolecules, separation of blood plasma occurs in the downstream part of the channel. Reproduced from Kar et al[58].

In principle, the design of paper-based 'H-filter' is different than usual paper-based filter matrix. In case of paper-based filter, filtration happens due to trapping of particles (or materials of interest) within the defined pores of the membrane, while in this case, the small molecules diffuse into the buffer (i.e. dilution phase) from the blood stream. Here, the porous matrix offers a support to the respective fluids to move forward by capillary action, while the pore dimensions do not play any significant role in actuating the separation of the blood plasma at the downstream part of the channel. Another key point to be noted here is that the 'H-filter' design offers the scope of integration of on-chip plasma separation module on microfluidic systems which is essentially required for point-of-care testing. Key limitation of this separation technique lies in incapability of dealing with large sample volume (typically not more than 50 microliter) and most importantly the separated plasma cannot be revived again from the device in liquid phase.

B. Green Energy Harvesting

To meet the quest of green energy harvesting, paper-based porous systems have been explored. Arun et al. have showed the use of paper-based fuel cells for a prolonged period (~1000 min) of energy generation.[64] In such a low-cost system, the maximum power density realized is ~32 mW/cm^2 at the cost of consumption of ~1 mL formic acid. In another work, Veerubhotla et al. demonstrated a frugal microbial fuel cell fabricated on cellulose based platform[65]. The device with its membrane-less design, works on continuously driven capillary mode, which uptakes oxygen from ambient to form water at the cathode and thereby promoting bioelectricity generation. This device uses two types of bacterial strains with the consequence of maximum induced potential of ~400 mV using Pseudomonas aeruginosa and maximum current of ~18 μA, with the aid of Shewanella putrefaciens bacteria.

Das et al. used paper-based devices as electrokinetic power generator[29] (shown in Figure 5). Due to the presence of free carboxylic acid and hydroxyl groups, cellulose fibers acquire net free negative charges on its surface while in contact with electrolyte (1 mM KCl) solution, which is confirmed by the measured zeta potential (-8.76 ± 0.7813 mV)[36]. Due to the generation of electrical double layer (EDL) on cellulose fibers, there will be surplus of counter ions in the

downstream part of the channel (i.e. towards the direction of flow) which essentially leads to the generation of streaming potential across the two ends of the device. Interestingly, this power generator works at virtually no expense, since the intrinsic capillary action of porous paper induces advective transport of ionic species for the establishment of the streaming potential. The capillary transport also sustains non-uniform distribution of ions, which essentially meets the need of constant power generation over a very long period of 12 days. A single device was able to generate a maximum output power of ~640 pW from a constant volume of ~50 µl KCl solution through capillarity-coupled-evaporation technique. The device performance was further enhanced up to ~100 times with the use of almost 20 array channel connection. In brief, it can be noted that the inherent capillary force of the tortuous paper network, which spontaneously triggers continuous re-distribution of the ionic species, leads to the power generation.

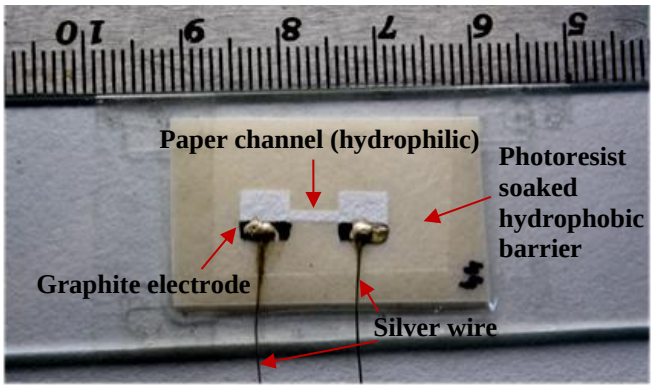

Figure 5: Paper-based hydroelectric power generator. Reproduced from Das et al[29].

Another important aspect of these porous networks is that it can be used as three-dimensional (3D) matrix, though in majority of the applications it is considered as 2D platform. The flexibility of designing it with customized thickness (by stacking of paper sheets) is an added advantage of these systems. Tao et al. has delineated the potential of the paper-based systems for cell culture applications as well, where it has shown enhanced cyto-compatibility[66]. The system was designed with a constant perfusion consideration by exploiting the intrinsic capillary action of paper. In this context, having accessibility to a 3D platform makes it more convenient for biological applications. Paper-based systems, available in wide variety of thicknesses (ranging from below 180 microns to 340 microns), provide the essential provision for using it as 3D system for cell culture applications.

6. Microfluidics on Silk Threads

Amongst other porous materials, silk-based threads are also gaining popularity[67]. Nilghaz et al. used silk-thread to characterize blood properties as well as blood typing[68]. The thread-based analytical devices are fabricated by properly selecting the thread morphology because the smooth surface of thread assists in easy migration of blood cell than the cotton surface. Banerjee et al. reported silk-based microfluidic chemical sensors[69]. Bhandari et al. used silk-yarns with different wettability for low-cost, and rapid medical diagnostics[70]. The device wicking rate as well as absorptivity capacity can be tuned further through yarn-twisting

frequency and weaving coverage area. Capillary flow through the yarn-fabric devices have been exploited for direct immunoassay using a polyclonal goat anti-rabbit immunoglobulin G (IgG) system. In another work, Tsioris et al. demonstrated silk yarn-based devices working on the principle of optofluidics, to detect pH[71]. The silk is chemically modified to improve pH sensitivity and further integrated with PDMS based device; and it yields a wide spectral pH response. Tao et al. demonstrated a silk-based sensor to detect food contaminants[72].

Recently, Das et al.[55] demonstrated a frugal technique of harvesting electrical power from a centimeter sized wet cotton fabric (Figure 6). The fabric-based channel is prepared from a wearable textile, which has three segments viz. root, stem and leaf, and therefore analogous to the transport system of a plant. In contrast to the existing electrokinetic energy generation technologies, the reported device uses surface energy, an intrinsic property of the fabric threads, to drive ions through the complex porous network (i.e. through the root and stem of the fabric based channel), and a bigger transpiration surface (i.e. leaf of fabric based channel) to achieve a continuous ion migration through natural evaporation of water. The developed technology is capable to generate a maximum of ~12 V electrical potential from multiple fabric-based channels connected in series configuration. The device can be further used for lighting white LEDs or for powering household mini-gadgets through combinatorial series-parallel connection. It thus culminates into a utilitarian scope of harvesting power in extremely rural areas, which may be extremely useful for point-care-diagnostics applications.

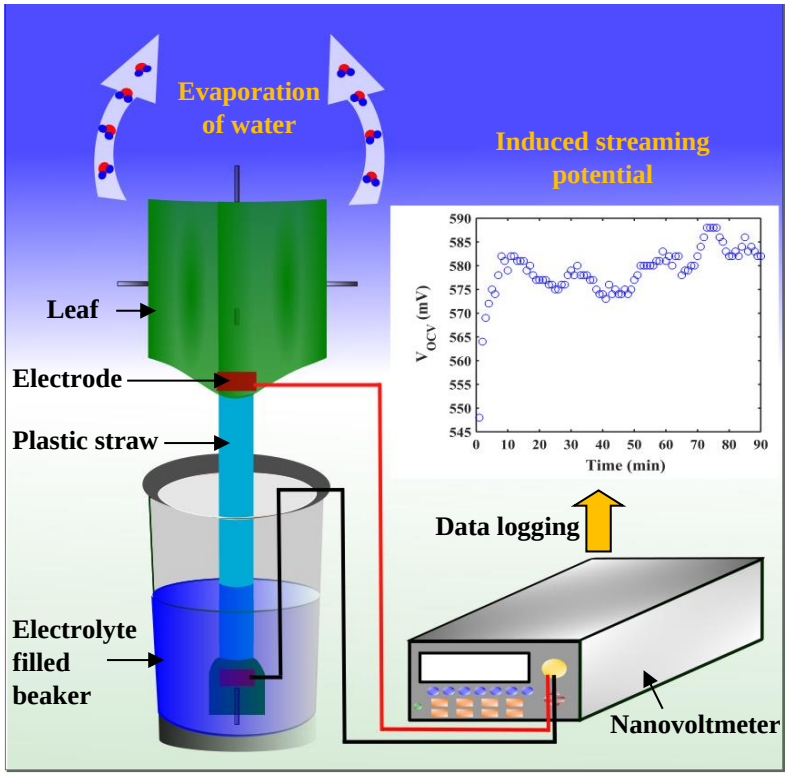

Figure 6: Fabric- (textile-)based electrokinetic power generator. Reproduced from Das et al.[55].

7. Conclusions and Outlook

In this short review, we emphasize that the physics of flow through complex porous networks can be understood with standard capillary-driven transport phenomena with certain pragmatic assumptions. Thus, the physical understanding of flow on these surfaces can be represented as a special case of standard capillary transport systems hallmarked by interfacial forces such as surface tension[73–84]. Furthermore, it is evident that the flexible manufacturing aspect of these porous systems certainly offers many key advantages of adopting it for investigating many complex fluidic phenomena with minimal expenses.

Here, we specifically focus on few key applications that are facilitated by the micro and nano-scale inhomogeneous distribution of particles, ions, small molecules, etc. and are actuated by simple capillarity driven flow through porous media without requiring any complex instrumentation. Key discussions concerning the specific platforms and the associated fabrication tools, influencing the fluid flow characteristics, can be summarized as follows:

1. From Figure 2, it is seen that the microscopic morphology of threads is significantly different from that of paper. Furthermore, the chemical composition of the underlying fabrics is also different from paper (for paper it is cellulose whilst in silk it is fibroin); which certainly affects the flow characteristics and different assays as well. Though the flow characteristics have been investigated for paper-based systems (both in experiments and theory) to some extent, the understanding of flow characteristics on thread-based systems has not yet been explored significantly. Further, short term liquid imbibition characteristics are yet to be realized in the true sense. It is understood that capillary action dominates for a very short initial regime of wicking in paper. Beyond this regime, the flow dynamics is mainly a diffusion dominated process. Further modelling efforts need to be directed towards capturing the underlying universal behavior.

2. Most of the fabrication techniques of paper-based devices can be adopted for low resource settings environment; however only few methods (e.g. photolithography) are able to produce very high-resolution structures. Furthermore, another key point associated with fabrication techniques and flow characteristics needs more careful attention. During the fabrication, entire paper surface is exposed to chemicals (except the techniques which involves usage of masks) and thereafter a cleaning step is employed to clean the chemicals from the undesired parts of the substrates. Due to the treatment of different chemicals in different fabrication methodologies, flow characteristics are affected in different manner. Though these microscopic alterations do not have any significant impact on chemicals-based assays, these will surely affect the fundamental transport phenomena on such substrates. This concern needs more careful attention while going forward towards the development of quantitatively accurate analytical devices. Further, there are few key operational aspects (e.g. valving, microscopy) which restricts the utilitarian scope as an alternative to high precision quantitative methods at par with the conventional glass, silicon-based systems.
3. Recent studies illustrate the successful integration of different actuation forces (e.g. electrical, surface acoustic waves) for improved efficacy of the devices. Further studies need to be directed towards obtaining a more comprehensive understanding of fluid flow through a complex fibrous porous network, under such complicated scenarios.

Acknowledgement:

The authors thank MHRD and ICMR, Government of India, for financial support through the IMPRINT programme. SC acknowledges the Department of Science and Technology, Government of India, for the Sir J. C. Bose National Fellowship.

References

(1) Kar, S.; Chakraborty, S. Evolution of Paper Microfluidics as an Alternate Diagnostic Platform. In *Paper Microfluidics: Theory and Applications*; Bhattacharya, S., Kumar, S., Agarwal, A. K., Eds.; Springer Singapore: Singapore, 2019; pp 83–98.

(2) Kar, S.; Maiti, T. K.; Chakraborty, S. Microfluidics-Based Low-Cost Medical Diagnostic Devices: Some Recent Developments. *Ina. Lett.* **2016**, *1*, 59.

(3) Martinez, A. W.; Phillips, S. T.; Butte, M. J.; Whitesides, G. M. Patterned Paper as a Platform for Inexpensive, Low-Volume, Portable Bioassays. *Angew. Chemie - Int. Ed.* **2007**, *46* , 1318.

(4) Martinez, A. W.; Phillips, S. T.; Whitesides, G. M. Diagnostics for the Developing World: Microfluidic Paper-Based Analytical Devices. *Anal. Chem.* **2010**, *82* , 3.

(5) Chen, G.-H.; Chen, W.-Y.; Yen, Y.-C.; Wang, C.-W.; Chang, H.-T.; Chen, C.-F. Detection of Mercury(II) Ions Using Colorimetric Gold Nanoparticles on Paper-Based Analytical Devices. *Anal. Chem.* **2014**, *86*, 6843.

(6) Rattanarat, P.; Dungchai, W.; Cate, D.; Volckens, J.; Chailapakul, O.; Henry, C. S. Multilayer Paper-Based Device for Colorimetric and Electrochemical Quantification of Metals. *Anal. Chem.* **2014**, *86*, 3555.

(7) Adkins, J. A.; Boehle, K.; Friend, C.; Chamberlain, B.; Bisha, B.; Henry, C. S. Colorimetric and Electrochemical Bacteria Detection Using Printed Paper-and Transparency-Based Analytic Devices. *Anal. Chem.* **2017**, *89*, 3613.

(8) Jokerst, J. C.; Adkins, J. A.; Bisha, B.; Mentele, M. M.; Goodridge, L. D.; Henry, C. S. Development of a Paper-Based Analytical Device for Colorimetric Detection of Select Foodborne Pathogens. *Anal. Chem.* **2012**, *84*, 2900.

(9) Mandal, P.; Dey, R.; Chakraborty, S. Electrokinetics with “paper-and-pencil” Devices. *Lab Chip* **2012**, *12* , 4026.

(10) Back to Basics Part 1: A Guide to Types of Whatman Filter Paper Grades. https://www.gelifesciences.com/en/us/solutions/lab-filtration/knowledge-center/a-guide-to-whatman-filter-paper-grades (accessed Jan 12, 2020).

(11) Washburn, E. W. The Dynamics of Capillary Flow. *Phys. Rev.* **1921**, *17*, 273.

(12) Lucas, R. Ueber Das Zeitgesetz Des Kapillaren Aufstiegs von Flüssigkeiten. *Kolloid-Zeitschrift* **1918**, *23*, 15.

(13) Zhmud, B. V.; Tiberg, F.; Hallstensson, K. Dynamics of Capillary Rise. *J. Colloid Interface Sci.* **2000**, *228*, 263.

(14) Chakraborty, S. Dynamics of Capillary Flow of Blood into a Microfluidic Channel. *Lab*

Chip **2005**, *5* , 421.

(15) Hoffman, R. L. A Study of the Advancing Interface. I. Interface Shape in Liquid-Gas Systems. *J. Colloid Interface Sci.* **1975** , *50* , 228.

(16) Kalliadasis, S.; Chang, H. C. Apparent Dynamic Contact Angle of an Advancing Gas-Liquid Meniscus. *Phys. Fluids* **1994,** *6* , 12.

(17) Ausserré, D.; Picard, A. M.; Léger, L. Existence and Role of the Precursor Film in the Spreading of Polymer Liquids. *Phys. Rev. Lett.* **1986,** *57* , 2671.

(18) Dhar, J.; Mukherjee, S.; Raj M, K.; Chakraborty, S. Universal Oscillatory Dynamics in Capillary Filling. *EPL* **2019**, *125*, 14003.

(19) Fu, E.; Ramsey, S. A.; Kauffman, P.; Lutz, B.; Yager, P. Transport in Two-Dimensional Paper Networks. *Microfluid. Nanofluid.* **2011,** *10*, 29.

(20) Chang, S.; Seo, J.; Hong, S.; Lee, D. G.; Kim, W. Dynamics of Liquid Imbibition through Paper with Intra-Fibre Pores. *J. Fluid Mech.* **2018**, *845*, 36.

(21) MacDonald, B. D. Flow of Liquids through Paper. *J. Fluid Mech.* **2018**, *852*, 1.

(22) Mendez, S.; Fenton, E. M.; Gallegos, G. R.; Petsev, D. N.; Sibbett, S. S.; Stone, H. A.; Zhang, Y.; López, G. P. Imbibition in Porous Membranes of Complex Shape: Quasi-Stationary Flow in Thin Rectangular Segments. *Langmuir* **2009**, *26*, 1380.

(23) Phillips, S. T.; Lewis, G. G. Advances in Materials That Enable Quantitative Point-of-Care Assays. *MRS Bull.* **2013**, *38*, 315.

(24) Walji, N.; MacDonald, B. D. Influence of Geometry and Surrounding Conditions on Fluid Flow in Paper-Based Devices. *Micromachines* **2016**, *7*, 73.

(25) Buser, J. R.; Byrnes, S. A.; Anderson, C. E.; Howell, A. J.; Kauffman, P. C.; Bishop, J. D.; Wheeler, M. H.; Kumar, S.; Yager, P. Understanding Partial Saturation in Paper Microfluidics Enables Alternative Device Architectures. *Anal. Methods* **2019**, *11*, 336.

(26) Buser, J. R. Heat, Fluid and Sample Control in Point-of-Care Diagnostics. Ph.D. Dissertation, University of Washington, USA. **2016**.

(27) Schuchard, D. R.; Berg, J. C. Liquid Transport in Composite Cellulose-Superabsorbent Fiber Networks. *Wood fiber Sci.* **1991**, *23* , 342.

(28) Masoodi, R.; Pillai, K. M. Darcy's Law-Based Model for Wicking in Paper-like Swelling Porous Media. *AIChE J.* **2010,** *56*, 2257.

(29) Das, S. S.; Kar, S.; Anwar, T.; Saha, P.; Chakraborty, S. Hydroelectric Power Plant on a Paper Strip. *Lab Chip* **2018**, *18* , 1560.

(30) Carrilho, E.; Martinez, A. W.; Whitesides, G. M. Understanding Wax Printing: A Simple Micropatterning Process for Paper-Based Microfluidics. *Anal. Chem.* **2009**, *81*, 7091.

(31) Nie, J.; Zhang, Y.; Lin, L.; Zhou, C.; Li, S.; Zhang, L.; Li, J. Low-Cost Fabrication of Paper-Based Microfluidic Devices by One-Step Plotting. *Anal. Chem.* **2012**, *84*, 6331.

(32) Bruzewicz, D. A.; Reches, M.; Whitesides, G. M. Low-Cost Printing of Poly(Dimethylsiloxane) Barriers to Define Microchannels in Paper. *Anal. Chem.* **2008**, *80*, 3387.

(33) Mani, N. K.; Prabhu, A.; Biswas, S. K.; Chakraborty, S. Fabricating Paper Based Devices Using Correction Pens. *Sci. Rep.* **2019**, *9* , 1.

(34) Maejima, K.; Tomikawa, S.; Suzuki, K.; Citterio, D. Inkjet Printing: An Integrated and Green Chemical Approach to Microfluidic Paper-Based Analytical Devices. *RSC Adv.* **2013**, *3* , 9258.

(35) Ruecha, N.; Chailapakul, O.; Suzuki, K.; Citterio, D. Fully Inkjet-Printed Paper-Based Potentiometric Ion-Sensing Devices. *Anal. Chem.* **2017**, *89*, 10608.

(36) Dey, R.; Kar, S.; Joshi, S.; Maiti, T. K.; Chakraborty, S. Ultra-Low-Cost 'Paper-and-Pencil' Device for Electrically Controlled Micromixing of Analytes. *Microfluid. Nanofluid.* **2015**, *19* , 375.

(37) Huang, G.-W.; Li, N.; Xiao, H.-M.; Feng, Q.-P.; Fu, S.-Y. A Paper-Based Touch Sensor with an Embedded Micro-Probe Array Fabricated by Double-Sided Laser Printing. *Nanoscale* **2017**, *9*, 9598.

(38) Olkkonen, J.; Lehtinen, K.; Erho, T. Flexographically Printed Fluidic Structures in Paper. *Anal. Chem.* **2010**, *82*, 10246.

(39) Garcia, P. D. T.; Cardoso, T. M. G.; Garcia, C. D.; Carrilho, E.; Coltro, W. K. . A Handheld Stamping Process to Fabricate Microfluidic Paper-Based Analytical Devices with Chemically Modified Surface for Clinical Assays. *RSC Adv.* **2014**, *4*, 37637.

(40) Fu, J.-Z.; He, Y.; Wu, W.-B. Rapid Fabrication of Paper-Based Microfluidic Analytical Devices with Desktop Stereolithography 3D Printer. *RSC Adv.* **2015**, *5*, 2694.

(41) Liu, N.; Xu, J.; An, H.-J.; Phan, D.-T.; Hashimoto, M.; Lew, W. S. Direct Spraying Method for Fabrication of Paper-Based Microfluidic Devices. *J. Micromech. Microeng.* **2017**, *27*, 104001.

(42) Cardoso, T. M.; De Souza, F. R.; Garcia, P. T.; Rabelo, D.; Henry, C. S.; Coltro, W. K. Versatile Fabrication of Paper-Based Microfluidic Devices with High Chemical Resistance Using Scholar Glue and Magnetic Masks. *Anal. Chim. Acta* **2017**, *974*, 63.

(43) Spicar-Mihalic, P.; Toley, B.; Houghtaling, J.; Liang, T.; Yager, P.; Fu, E. CO2 Laser Cutting and Ablative Etching for the Fabrication of Paper-Based Devices. *J. Micromech. Microeng.* **2013**, *23*, 067003.

(44) Das, S. S.; Kar, S.; Dawn, S.; Saha, P.; Chakraborty, S. Electrokinetic Trapping of Microparticles Using Paper-and-Pencil Microfluidics. *Phys. Rev. Appl.* **2019**, *10* , 1.

(45) Mani, N. K.; Das, S. S.; Dawn, S.; Chakraborty, S. Electro-Kinetically Driven Route for Highly Sensitive Blood Pathology on a Paper-Based Device. *Electrophoresis*. **2020**, 1.

(46) Songok, J.; Toivakka, M. Enhancing Capillary-Driven Flow for Paper-Based Microfluidic Channels. *ACS Appl. Mater. Interfaces* **2016**, *8* , 30523.

(47) Apilux, A.; Ukita, Y.; Chikae, M.; Takamura, O. C. and Y. Development of Automated Paper-Based Devices for Sequential Multistep Sandwich Enzyme-Linked Immunosorbent Assays Using Inkjet Printing. *Lab Chip* **2013**, *13*, 126.

(48) Songok, J.; Toivakka, M. Controlling Capillary-Driven Surface Flow on a Paper-Based Microfluidic Channel. *Microfluid. Nanofluid.* **2016** , *20*, 63.

(49) Younas, M.; Maryam, A.; Khan, M.; Nawaz, A. A.; Jaffery, S. H. I.; Anwar, M. N.; Ali,

L. Parametric Analysis of Wax Printing Technique for Fabricating Microfluidic Paper-Based Analytic Devices (MPAD) for Milk Adulteration Analysis. *Microfluid. Nanofluid.* **2019**, *23* , 1.

(50) Hong, S.; Kim, W. Dynamics of Water Imbibition through Paper Channels with Wax Boundaries. *Microfluid. Nanofluid.* **2015**, *19*, 845.

(51) Ghanbarian, B.; Hunt, A. G.; Ewing, R. P.; Sahimi, M. Tortuosity in Porous Media: A Critical Review. *Soil Sci. Soc. Am. J.* **2013**, *77* , 1461.

(52) Koponen, A.; Kataja, M.; Timonen, J. Tortuous Flow in Porous Media. *Phys. Rev. E - Stat. Physics, Plasmas, Fluids, Relat. Interdiscip. Top.* **1996**, *54* , 406.

(53) Gruener, S.; Huber, P. Imbibition in Mesoporous Silica: Rheological Concepts and Experiments on Water and a Liquid Crystal. *J. Phys. Condens. Matter* **2011**, *23*, 184109.

(54) Li, T.; Li, S. X.; Kong, W.; Chen, C.; Hitz, E.; Jia, C.; Dai, J.; Zhang, X.; Briber, R.; Siwy, Z.; et al. A Nanofluidic Ion Regulation Membrane with Aligned Cellulose Nanofibers. *Sci. Adv.* **2019**, *5* , 1.

(55) Das, S. S.; Manaswi, V. P. A. B.; Saha, P.; Chakraborty, S. Electrical Power Generation from Wet Textile Mediated by Spontaneous Nanoscale Evaporation. *Nano Lett.* **2019**, *19* , 7191.

(56) Ceratti, D. R.; Faustini, M.; Sinturel, C.; Vayer, M.; Dahirel, V.; Jardat, M.; D. Grosso. Critical Effect of Pore Characteristics on Capillary Infiltration in Mesoporous Films. *Nanoscale* **2015**, *7*, 5371.

(57) Chaudhury, K.; Kar, S.; Chakraborty, S. Diffusive Dynamics on Paper Matrix. *Appl. Phys. Lett.* **2016**, *109* , 224101.

(58) Kar, S.; Maiti, T. K.; Chakraborty, S. Capillarity-Driven Blood Plasma Separation on Paper-Based Devices. *Analyst* **2015**, *140* , 6473.

(59) Songjaroen, T.; Dungchai, W.; Chailapakul, O.; Laiwattanapaisal, C. S. H. and W. Blood Separation on Microfluidic Paper-Based Analytical Devices. *Lab Chip* **2012**, *12*, 3392.

(60) Yang, X.; Forouzan, O.; Shevkoplyas, T. P. B. and S. S. Integrated Separation of Blood Plasma from Whole Blood for Microfluidic Paper-Based Analytical Devices. *Lab Chip* **2012**, *12*, 274.

(61) Azadeh Nilghaz and Wei Shen. Low-Cost Blood Plasma Separation Method Using Salt Functionalized Paper. *RSC Adv.* **2015**, *5*, 53172.

(62) Noiphung, J.; Songjaroen, T.; Dungchai, W.; S.Henry, C.; Orawon Chailapakul, A.; Laiwattanapaisal, W. Electrochemical Detection of Glucose from Whole Blood Using Paper-Based Microfluidic Devices. *Anal. Chim. Acta* **2013**, *788*, 39.

(63) Osborn, J. L.; Lutz, B.; Fu, E.; Kauffman, P.; Yagera, D. Y. S. and P. Microfluidics without Pumps: Reinventing the T-Sensor and H-Filter in Paper Networks. *Lab Chip* **2010**, *10*, 2659.

(64) Arun, R. K.; Halder, S.; Chanda, N.; Chakraborty, S. A Paper Based Self-Pumping and Self-Breathing Fuel Cell Using Pencil Stroked Graphite Electrodes. *Lab Chip* **2014**, *14*, 1661.

(65) Veerubhotla, R.; Bandopadhyay, A.; Das, D.; Chakraborty, S. Instant Power Generation

from an Air-Breathing Paper and Pencil Based Bacterial Bio-Fuel Cell. *Lab Chip* **2015**, *15*, 2580.

(66) Tao, F. F.; Xiao, X.; Lei, K. F.; Lee, I. C. Paper-Based Cell Culture Microfluidic System. *Biochip J.* **2015**, *9* , 97.

(67) Safavieh, R.; Gina Z. Zhoua and David Juncker. Microfluidics Made of Yarns and Knots: From Fundamental Properties to Simple Networks and Operations. *Lab Chip* **2011**, *11*, 2618.

(68) Nilghaz, A.; Wicaksono, D. H. B.; Gustiono, D.; Abdul Majid, F. A.; Supriyanto, E.; Abdul Kadir, M. R. Flexible Microfluidic Cloth-Based Analytical Devices Using a Low-Cost Wax Patterning Technique. *Lab Chip* **2012**, *12* , 209.

(69) Banerjee, S. S.; Roychowdhury, A.; Taneja, N.; Janrao, R.; Khandare, J.; Paul, D. Chemical Synthesis and Sensing in Inexpensive Thread-Based Microdevices. *Sensors Actuators, B Chem.* **2013**, *186*, 439.

(70) Bhandari, P.; Narahari, T.; Dendukuri, D. Fab-Chips: A Versatile, Fabric-Based Platform for Low-Cost, Rapid and Multiplexed Diagnostics. *Lab Chip* **2011**, *11* , 2493.

(71) Tsioris, K.; Tilburey, G. E.; Murphy, A. R.; Domachuk, P.; Kaplan, D. L.; Omenetto, F. G. Functionalized-Silk-Based Active Optofluidic Devices. *Adv. Funct. Mater.* **2010**, *20* , 1083.

(72) Tao, H.; Brenckle, M. A.; Yang, M.; Zhang, J.; Liu, M.; Siebert, S. M.; Averitt, R. D.; Mannoor, M. S.; McAlpine, M. C.; Rogers, J. A.; et al. Silk-Based Conformal, Adhesive, Edible Food Sensors. *Adv. Mater.* **2012**, *24* , 1067.

(73) Bandopadhyay, A.; Tripathi, D.; Chakraborty, S. Electroosmosis-Modulated Peristaltic Transport in Microfluidic Channels. *Phys. Fluids* **2016**, *28* , 052002.

(74) Das, S.; Chakraborty, S.; Mitra, S. K. Redefining Electrical Double Layer Thickness in Narrow Confinements: Effect of Solvent Polarization. *Phys. Rev. E* **2012**, *85* , 051508.

(75) Garai, A.; Chakraborty, S. Steric Effect and Slip-Modulated Energy Transfer in Narrow Fluidic Channels with Finite Aspect Ratios. *Electrophoresis* **2010**, *31* , 843.

(76) Chakraborty, S.; Ray, S. Mass Flow-Rate Control through Time Periodic Electro-Osmotic Flows in Circular Microchannels. *Phys. Fluids* **2008**, *20*, 083602.

(77) Kate, R. P.; Das, P. K.; Chakraborty, S. Hydraulic Jumps Due to Oblique Impingement of Circular Liquid Jets on a Flat Horizontal Surface. *J. Fluid Mech.* **2007**, *573*, 247.

(78) Chakraborty, S.; Som, S. K. Heat Transfer in an Evaporating Thin Liquid Film Moving Slowly Along the Walls of an Inclined Microchannel. *Int. J. Heat Mass Transf.* **2005**, *48*, 2801.

(79) Das, S.; Das, T.; Chakraborty, S. Analytical Solutions for the rate of DNA Hybridization in a Microchannel in the Presence of Pressure-driven and Electroosmotic Flows. *Sensors Actuators, B Chem.* **2006**, *114*, 957.

(80) Das, S.; Chakraborty, S. Transverse Electrodes for Improved DNA Hybridization in Microchannels. *AIChE J.* **2007**, *53*, 1086.

(81) Das, S. P., Chakraborty, S.; Dutta, P. Studies on Thermal Stratification Phenomenon in LH2 Storage Vessel. *Heat Transf. Eng.* **2004**, *25*, 54.

(82) Chakraborty, S. Towards a Generalized Representation of Surface Effects on Pressure-driven Liquid Flow in Microchannels. *Appl. Phys. Lett.* **2007**, *90*, 034108.

(83) Sarkar, S. Raj; P. M.; Chakraborty, S.; Dutta, P. Three-dimensional Computational Modeling of Momentum, Heat, and Mass Transfer in a Laser Surface Alloying Process. *Numer. Heat Transf. Part A Appl.* **2002**, *42*, 307.

(84) Raj, P. M.; Sarkar, S.; Chakraborty, S.; Phanikumar; G., Dutta, P. Modelling of Transport Phenomena in Laser Surface Alloying with Distributed Species Mass Source. *Int. J. Heat Fluid Flow* **2002**, *23*, 298.

For Table of Contents Only